

Ubiquitin-proteasome-dependent proteolytic activity remains elevated after zymosan-induced sepsis in rats while muscle mass recovers

R. Minnaard^{a,*}, A.J.M. Wagenmakers^b, L. Combaret^c, D. Attaix^c,
M.R. Drost^a, G.P. van Kranenburg^a, G. Schaart^a, M.K.C. Hesselink^a

^a Nutrition and Toxicology Research Institute Maastricht (NUTRIM), Department of Movement Sciences, Maastricht University, P.O. Box 616, 6200 MD Maastricht, The Netherlands

^b School of Sport and Exercise Sciences, University of Birmingham, Birmingham, UK

^c Nutrition and Protein Metabolism Unit, Institut National de la Recherche Agronomique, Ceyrat, France

Received 10 March 2005; received in revised form 29 April 2005; accepted 3 May 2005

Abstract

We studied the role of the ubiquitin-proteasome system in rat skeletal muscle during sepsis and subsequent recovery. Sepsis was induced with intraperitoneal zymosan injections. This model allows one to study a sustained and reversible catabolic phase and mimics the events that prevail in septic and subsequently recovering patients. In addition, the role of the ubiquitin-proteasome system during muscle recovery is poorly documented. There was a trend for increased ubiquitin-conjugate formation in the muscle wasting phase, which was abolished during the recovery phase. The trypsin- and chymotrypsin-like peptidase activities of the 20S proteasome peaked at day 6 following zymosan injection (i.e. when both muscle mass and muscle fiber cross-sectional area were reduced the most), but remained elevated when muscle mass and muscle fiber cross-sectional area were recovering (11 days). This clearly suggests a role for the ubiquitin-proteasome pathway in the muscle remodeling and/or recovery process. Protein levels of 19S complex and 20S proteasome subunits did not increase throughout the study, pointing to alternative mechanisms regulating proteasome activities. Overall these data support a role for ubiquitin-proteasome dependent proteolysis in the zymosan septic model, in both the catabolic and muscle recovery phases.

© 2005 Elsevier Ltd. All rights reserved.

Keywords: Muscle; Atrophy; Sepsis; Ubiquitin; Proteasome

1. Introduction

In many catabolic conditions exhibiting extensive muscle wasting (e.g. starvation, cancer, sepsis, renal failure, etc.) increased proteolysis occurs largely

* Corresponding author. Tel.: +31 43 3881394;
fax: +31 43 3670972.

E-mail address: Ronnie.Minnaard@bw.unimaas.nl
(R. Minnaard).

through the ubiquitin-proteasome (Ub-P) pathway (Attaix, Combaret, Kee, & Taillandier, 2003; Jagoe & Goldberg, 2001). This ATP-dependent proteolytic pathway can be divided into two major steps. In the first step, proteins are targeted for degradation by covalent attachment of a polyubiquitin chain (ubiquitin conjugation). Ubiquitin conjugation is achieved by the combined action of the Ub-activating enzyme (E1), Ub-conjugating enzymes (E2) and Ub-ligases (E3) (Pickart, 2001). In the second step, ubiquitinated proteins are recognized and degraded by the 26S proteasome, a large multi-catalytic protein complex, which comprises two 19S regulatory complexes and a 20S proteolytic core. Multiple catabolic conditions, such as sepsis, cancer and diabetes, are typified by activation of a series of Ub-P related events, like increased ubiquitin conjugation rates (Lecker, Solomon, & Mitch, 1999; Solomon, Baracos, Sarraf, & Goldberg, 1998), increased levels of mRNA encoding for key components of the system (Attaix et al., 2003; Lecker et al., 2004; Price, 2003) and increased proteasome activity (Combaret et al., 2004; Hobler et al., 1999).

Acute models of sepsis like cecal ligation and puncture (CLP) and endotoxin injections, commonly used to induce experimental sepsis in animals, result either in premature death or in a very transient catabolic state. As a consequence, most of the information on the regulation of the Ub-P system during sepsis applies only to the acute phase. Therefore, it is not possible to investigate the period of recovery following acute sepsis. Intraperitoneal zymosan injections have been used in rats to investigate the effects of an acute sepsis followed by a recovery period that includes a restoration of food intake and muscle mass (Rooyackers, Saris, Soeters, & Wagenmakers, 1994). As the muscle atrophy in this model is more sustained and reversible, this model better resembles the events that prevail in septic and subsequently recovering patients than the CLP and endotoxin models. Zymosan is a potent stimulator of the alternative pathway of the complement system and of macrophages. Intraperitoneal injections with zymosan result in an acute local inflammatory response (peritonitis), triggering a systemic response resulting in clinical sepsis. Zymosan injection results in acute sepsis followed by a prolonged recovery. Signs of catabolism (reduction of body and muscle mass) are present until 6 days after zymosan injection. For a full comprehension of the role of the Ub-P system

during acute sepsis-induced atrophy and subsequent muscle mass recovery, it is of importance to study the time-course of the Ub-P system response. Therefore, the aim of this study was to measure changes in protein content of key components of the Ub-P system, ubiquitin-conjugate formation and proteasome activities both during the acute wasting phase of sepsis and the subsequent recovery period.

It was anticipated that increased formation of ubiquitin-conjugates, increased (specific) proteasome activity and increased protein levels of the 19S and 20S proteasome subunits would be most prominent in the period of rapid muscle wasting in the first days after zymosan injection and would return to control levels in the period of muscle mass recovery. Comparisons are made with pair-fed control rats to discriminate between the effects of sepsis on the one hand, and of reduced food intake on the other hand.

2. Materials and methods

2.1. Animals and experimental design

The experiments were approved by the institutional animal experimental committee. Rats were individually housed (12 h dark/12 h light cycle, 21–22 °C and 50–60% humidity). Zymosan was used according to Rooyackers et al. (1994). Ten-week-old, male Wistar rats with a body mass of 300 ± 24 g were randomly assigned to a zymosan-injected, a pair-fed or an ad libitum fed control group. Rats assigned to the zymosan group were given an aseptic intraperitoneal injection of zymosan (30 mg/100 g body mass, homogeneously suspended in liquid paraffin (25 mg/ml)), based on pilot studies with a mortality rate of approximately 20%. Pilot experiments testing the effect of an i.p. injection with sterile paraffin did not show any effect on food intake and body weight during an 11-day follow-up. We interpreted this as the absence of a 'vehicle' effect. Four groups of rats ($n = 10$) were injected with this zymosan suspension. Food intake and body mass were recorded daily. At 2 h, 2, 6 and 11 days after zymosan injection the main dorsi- and plantar flexor muscles of the hindlimb (tibialis anterior (TA) and gastrocnemius, respectively) were carefully dissected under isoflurane anesthesia, weighed (wet weight) and frozen in melting 2-methylbutane, after which rats were sacri-

ficed by cervical dislocation. Since zymosan injection affects food intake, control rats were pair-fed to the 2, 6 and 11 days zymosan rats. An ad libitum fed control group, which was sacrificed at day 11, was also included.

2.2. Muscle fiber cross-sectional area quantitation

The mean TA muscle fiber cross-sectional area (CSA) was determined as described recently (Minnaard et al., 2005). Briefly, transverse muscle sections were cut and incubated with a rabbit polyclonal laminin antibody (Sigma, Zwijndrecht, The Netherlands), followed by incubation with an Alexa350-conjugated goat anti-rabbit Ig antibody (Molecular Probes, Invitrogen, Breda, The Netherlands). Muscle fiber CSA was quantitated using a fluorescence microscope (Uvikon, Bunnik, The Netherlands) and Lucia 4.8 software (Nikon, Düsseldorf, Germany) using the laminin signal as a marker for cell boundary.

2.3. Western blot analysis

Individual tibialis anterior muscles were homogenized in 4 ml ice-cold buffer (pH 7.5), containing 50 mM Tris, 1 mM EDTA, 1 mM DTT, 1 mM PMSF, 10 µg/ml pepstatin A and 10 µg/ml leupeptin. Homogenates were centrifuged at $10,000 \times g$, 4 °C for 10 min and the resulting supernatants were centrifuged at $100,000 \times g$, 4 °C for 1 h. The soluble protein concentration was determined in the supernatant using the Bio-Rad protein assay. Soluble proteins (20 µg) were subjected to routine Western blotting using 12% polyacrylamide SDS-gels and antibodies against the 14-kDa E2 (polyclonal rabbit antibody; 1:5000), the 19S complex subunit S6a (TBP1-19; monoclonal mouse antibody; 1:10,000; Affiniti Research Products, Exeter, UK) and the 20S proteasome subunit C8 (MCP72; mouse monoclonal; 1:10,000; Affiniti). After washing, blots were incubated with either a horseradish peroxidase-conjugated swine anti-rabbit Ig (SwARPO, DAKO, Glostrup, Denmark) or a horseradish peroxidase-conjugated rabbit anti-mouse Ig (DAKO), both diluted 1:10,000. Chemiluminescence was performed using a Super Signal West Dura extended kit (Pierce, Rockford, IL) and the blots were exposed to CL-Xposure Film (Pierce). Protein bands were quantified using optical densitometry.

2.4. Ubiquitin-conjugate formation

Soluble proteins were prepared from individual TA muscles as described in the Western blot section, after which they were pooled ($n = 10$ per group). The ubiquitin-conjugate formation was determined by incubating 50 µg of soluble proteins for 1 h at 37 °C with 5 µM [125 I]-labelled ubiquitin (specific activity ~3000 cpm/pmol), 50 mM Tris-HCl (pH 7.5), 1 mM DTT, 2 mM MgCl₂ and 2 mM AMP-PNP, in a total volume of 20 µl. The reactions were stopped by adding 1 × sample buffer according to Laemmli (1970) (62.5 mM Tris-HCl (pH 6.8), 5% β-mercaptoethanol, 2% SDS, 0.1% bromophenol blue and 10% glycerol). It has been shown that conjugation rates are linear for these 60 min and that exogenous labelled ubiquitin was present in significant excess of any endogenous ubiquitin (i.e. addition of higher amounts of labelled ubiquitin did not increase rates of ubiquitin conjugation) (Kee et al., 2003). After stopping the reaction, the ubiquitin-conjugated proteins were separated from free ubiquitin by electrophoresis on 12% polyacrylamide SDS-gels. Subsequently, gels were dried and exposed to Hyperfilm MP (Amersham Biosciences, Roosendaal, The Netherlands). The film was scanned and both the high molecular weight conjugate band and the 70 kDa ubiquitin-conjugate band were quantified by optical densitometry.

2.5. Isolation of 20S proteasomes and measurement of peptidase activities

In all groups the 20S proteasome activities were determined in the gastrocnemius lateralis muscle essentially according to Hobler et al. (1999). Briefly, muscles were homogenized and proteasomes were isolated by sequential (ultra)centrifugation steps. Proteasome fractionation yielded similar amounts of protein (determined with the Bio-Rad protein assay) across the different experimental groups. The peptidase activities of the 20S proteasome were determined fluorometrically by measuring the hydrolysis of the fluorogenic substrates succinyl-Leu-Leu-Val-Tyr-7-amido-4-methylcoumarin (Suc-LLVY-AMC, Sigma) and *t*-butoxycarbonyl-Leu-Arg-Arg-7-amido-4-methylcoumarin (Boc-LRR-AMC, Affiniti). These substrates are preferentially hydrolyzed by the chymotrypsin- and trypsin-like activities of the 20S

proteasome, respectively. Standard curves were established for AMC, which permitted the expression of the proteasome activity as pmol AMC/ μ g protein/min. Adding the proteasome inhibitor MG132 to the reaction resulted in complete inhibition of the proteasome peptidase activities.

2.6. Statistics

Results are presented as mean \pm S.E.M. To study the effects of zymosan injection and pair-feeding on the measured parameters in time a one-way ANOVA was performed using ad libitum fed control data as $t = 0$ data. Differences were located using the Scheffé post-hoc test. Two-way ANOVA was performed to examine the interaction between intervention (zymosan treatment or pair-feeding) and time. Significance was set at $P < 0.05$.

3. Results

3.1. Characterization of the zymosan model

Zymosan injection induced an acute peritonitis, with symptoms of severe illness being present in all rats during the first 2 days after injection. Symptoms included lethargy, hypophagia, hyperventilation, tachycardia, fever, diarrhea and loss of hemorrhagic fluid from the nose. As anticipated, zymosan injection resulted in 20% mortality. Fig. 1A shows a reduction of food intake of approximately 90% until 2 days post-injection with a gradual increase of food intake towards day 7. Hereafter, food intake remained stable, but at a significantly lower level ($\sim 18\%$) than in controls. The reduced food intake was almost instantaneously reflected in a decreased body mass, with a similar response being present in the zymosan and pair-fed control rats (Fig. 1B).

As soon as 2 days after zymosan injection, the mass (Fig. 2) and fiber CSA (Table 1) of the TA muscle declined significantly compared to both pair-fed and ad libitum fed controls. The most prominent decline was observed at day 6. The pair-fed group showed similar, albeit less pronounced responses for both muscle mass and fiber CSA. On day 11, the TA muscle mass was increased compared to day 6 in both the zymosan-treated ($P = 0.008$) and pair-fed

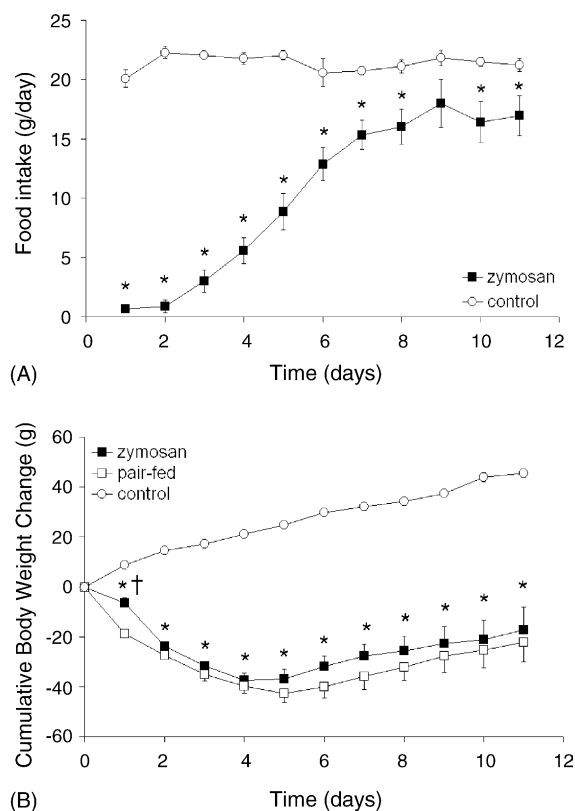


Fig. 1. (A) Food intake of zymosan-treated and ad libitum fed control rats. (B) Cumulative body weight change in the experimental groups. * $P < 0.05$ compared to ad libitum fed control rats. † $P < 0.05$ vs. pair-fed rats.

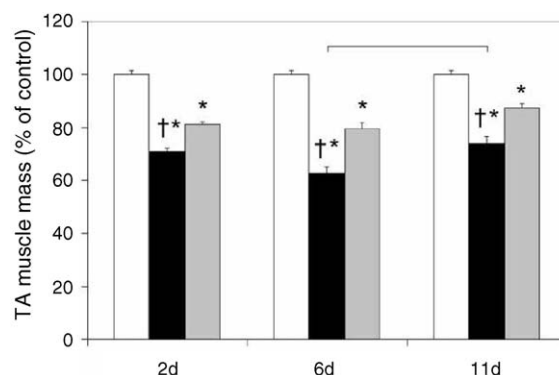


Fig. 2. Tibialis anterior muscle mass (percent of control absolute muscle mass) at different time points in zymosan (black bars), pair-fed (grey bars) and ad libitum fed control (white bars) rats. * $P < 0.05$ vs. ad libitum fed control rats. † $P < 0.05$ vs. pair-fed rats. No intervention \times time effect was detected. The bracket indicates a significant difference between the 6- and 11-day zymosan-treated groups.

Table 1
Muscle fiber cross-sectional area (CSA) in the Tibialis anterior

Group	Mean fiber CSA (μm^2)
Control	1469 \pm 70
2-day zymosan	1108 \pm 69 (–25%)*,†
2-day pair-fed	1351 \pm 81 (–8%)
6-day zymosan	1009 \pm 62 (–31%)*,†
6-day pair-fed	1264 \pm 83 (–14%)*
11-day zymosan	1163 \pm 70 (–21%)*,†
11-day pair-fed	1363 \pm 59 (–7%)

Values between brackets indicate the relative reduction of CSA vs. ad libitum fed controls.

* $P < 0.05$ vs. ad libitum fed control rats.

† $P < 0.05$ vs. pair-fed controls.

groups ($P = 0.016$). The TA fiber CSA showed the same trends in both the zymosan-treated and pair-fed groups, although the 6 and 11 days values were not significantly different. The same pattern of wasting and recovery was observed in the gastrocnemius muscle (data not shown).

3.2. Ubiquitin-conjugate formation

The in vitro formation of ubiquitin-conjugates increased (+50%) within 2 h after zymosan injection (Fig. 3), transiently decreased at day 2, peaked again at day 6 (+49%) and was totally normalized at day 11. Except for day 2 (+35%), there was no increased accumulation of ubiquitin-conjugates in the pair-fed rats.

3.3. Protein levels of components of the ubiquitin-proteasome pathway

To examine if changes in ubiquitin-conjugate formation and proteasome activity can be explained by changes in protein levels of key components of the Ub-P system, we determined protein levels of the 14-kDa E2 ubiquitin conjugating enzyme, the 19S complex S6a subunit and the 20S proteasome C8 subunit at days 2, 6 and 11. A significant increase in 14-kDa E2 protein levels (compared to controls) was only observed 2 days after zymosan injection (Fig. 4A). The protein levels of the 19S complex subunit S6a (Fig. 4B) and 20S proteasome subunit C8 (Fig. 4C) did not change in either the zymosan-injected or pair-fed rats.

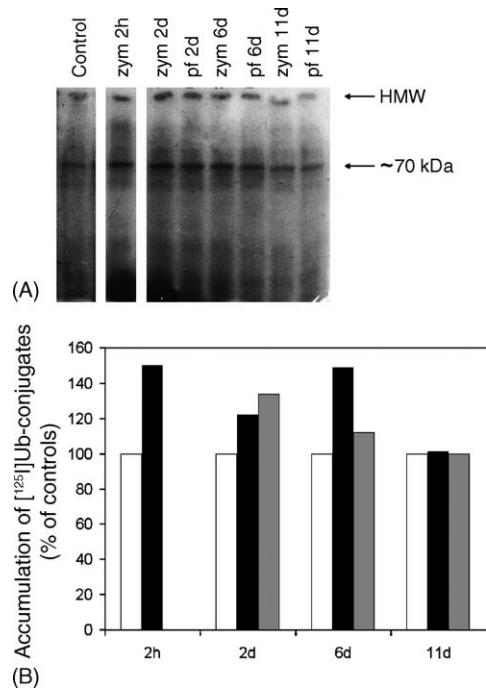


Fig. 3. (A) Accumulation of soluble muscle [^{125}I]Ub-conjugates in the control, zymosan-injected (zym) and pair-fed (pf) groups. HMW denotes high molecular weight proteins. (B) Quantitation of [^{125}I]Ub-conjugation (% of controls) in zymosan-injected (black bars), pair-fed (grey bars) and ad libitum fed control (white bars) rats. Values are averages of three separate measurements.

3.4. 20S Proteasome activities

The trypsin-like peptidase activity of the 20S proteasome markedly increased (+47%) as early as 2 h after zymosan injection and remained elevated throughout the study (Fig. 5B). The chymotrypsin- and trypsin-like peptidase activities of the 20S proteasome increased by 82 and 100% at day 6 after zymosan injection, respectively, when the decline in muscle mass was most prominent. The trypsin-like activity was markedly and significantly higher in the zymosan than in the pair-fed group at all time-points, while the chymotrypsin-like activity was markedly higher at days 6 and 11. Notably, the peptidase activities of the 20S proteasome (either trypsin- or chymotrypsin-like) did not exceed control values in the pair-fed groups, except for the trypsin-like activity at day 11. While at day 11 muscle mass is increased in comparison to day 6 ($P = 0.008$), the 20S

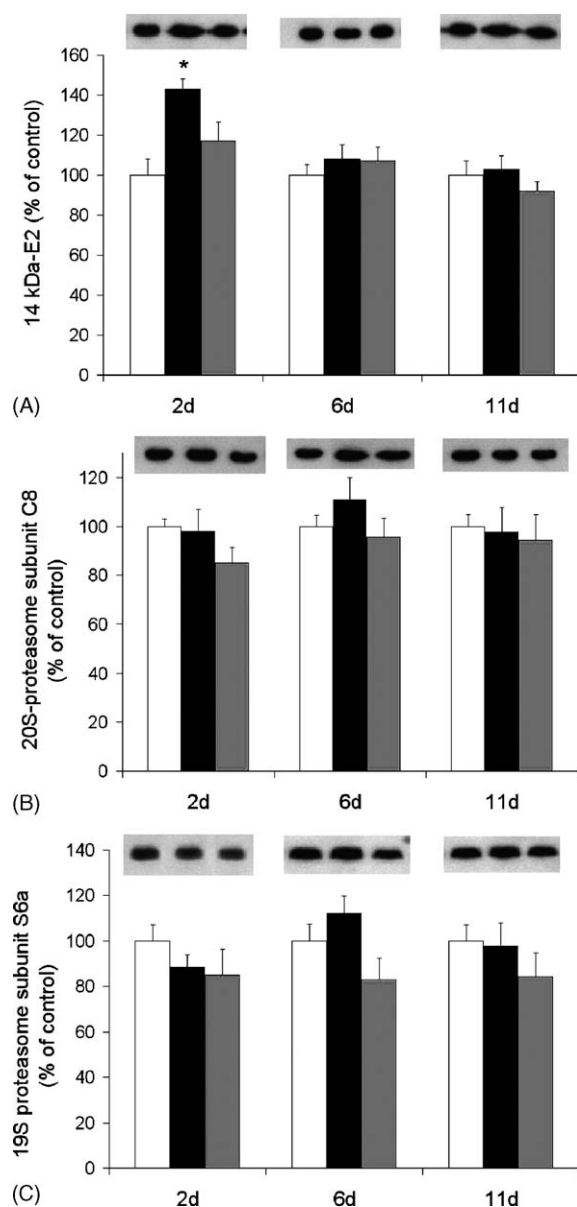


Fig. 4. Protein levels (% of controls) of (A) the 14-kDa-E2 ubiquitin-conjugating enzyme, (B) subunit S6a of the 19S complex and (C) 20S proteasome subunit C8, at several time points in zymosan-injected (black bars), pair-fed (grey bars) and ad libitum fed (white bars) rats. * $P < 0.05$ vs. ad libitum fed control rats. No treatment \times time effect was detected.

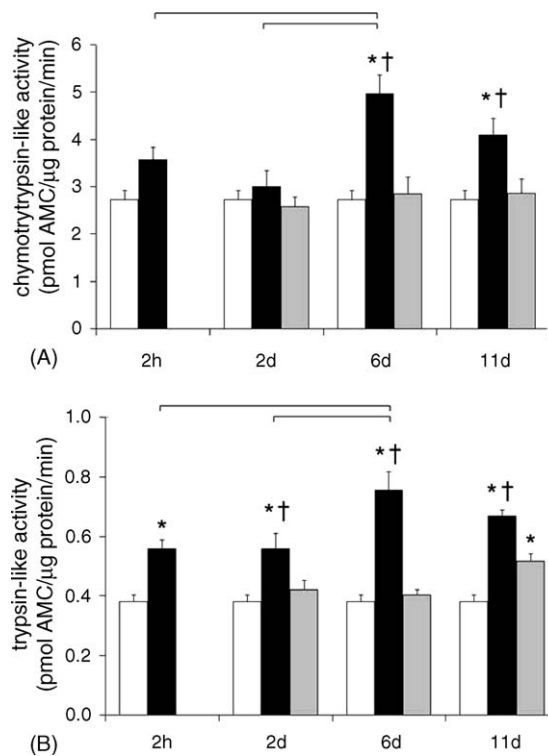


Fig. 5. (A) Chymotrypsin- and (B) trypsin-like peptidase activities of the 20S proteasome (expressed as pmol AMC/μg protein/min) at several time points in zymosan-injected (black bars), pair-fed (grey bars) and ad libitum fed (white bars) rats. * $P < 0.05$ vs. ad libitum fed control rats. † $P < 0.05$ vs. pair-fed rats. A significant treatment \times time effect was detected for the chymotrypsin ($P = 0.045$) and trypsin-like ($P = 0.012$) peptidase activities of the 20S proteasome. The brackets denote significant differences between the respective zymosan-injected groups.

proteasome peptidase activities remained high in the zymosan-injected group at this time point.

4. Discussion

In the present study, sepsis-induced muscle wasting was achieved by intraperitoneal injection with zymosan, resulting in a period of acute sepsis. Although zymosan-induced sepsis is primarily caused by a non-infective stimulus rather than by the actual presence of bacteria, classical infectious responses (e.g. tachycardia, fever, increased respiratory rate and hypophagia) were observed. Throughout the 11-day period of inves-

tigation body and muscle mass of the zymosan-injected rats had not yet returned to control values. Using this model we observed both acute (within 2 h) and prolonged effects on the Ub-P pathway, i.e. trends for increased ubiquitin-conjugation formation for up to 6 days, increased chymotrypsin-like activity at days 6 and 11, and increased trypsin-like activities of the 20S proteasome throughout the study. Notably, these changes were not paralleled by increased protein levels of subunits of both the 19S complex and 20S proteasome. These data suggests that proteasome activities may be upregulated by alternative mechanisms. At day 11, when muscle mass was clearly recovering, the 20S proteasome peptidase activities were still significantly elevated. This observation is remarkable and clearly suggests that in the recovery period, when muscle mass recovers, the degradation rate of at least a number of proteins is upregulated. Another striking observation was that the decreased muscle mass in the pair-fed rats did not require significant increases in peptidase activities of the 20S proteasome. Thus, muscle wasting during periods of reduced food intake in otherwise healthy rats was not accompanied by marked effects on the Ub-P system.

The increased ubiquitin-conjugate formation in the zymosan septic model is in agreement with previous observations in other catabolic conditions, including fasting (Kee et al., 2003), cancer (Solomon et al., 1998), diabetes (Lecker et al., 1999b) and dexamethasone treatment (Combaret et al., 2004). However, care should be taken in interpreting our results, as we measured the accumulation of Ub-conjugates at a single time point and not the rate of ubiquitination. Whereas it had been shown that following CLP rates of ubiquitin conjugation were increased within 16 h after induction of sepsis (Solomon et al., 1998), the present data suggest that the formation of ubiquitin-conjugates increased as early as 2 h after inducing sepsis.

Increased mRNA levels of subunits of the 20S proteasome are commonly observed in multiple catabolic conditions, including sepsis, in both rat (Chai, Wu, & Sheng, 2002; Deval et al., 2001; Hobler et al., 1999; Voisin et al., 1996) and human muscles (Tiao et al., 1997). Similar observations also prevailed for 19S proteasome subunits in other catabolic conditions (Price, 2003). This study clearly shows that, despite the previously reported responsiveness to catabolic conditions of subunits of the 19S complex and the 20S protea-

some at the mRNA level, changes at the protein level were absent. This suggests that it is premature to link increased mRNA levels of proteasome subunits directly to increased proteasome activity and increased rates of proteolysis. In line with this, administering glucocorticoids to induce muscle atrophy in rats increased proteasome activity and mRNA levels of five 19S proteasome subunits, while protein levels of these subunits did not change (Combaret et al., 2004). Also, CLP-induced sepsis in rats upregulated the 20S proteasome C9 subunit mRNA level without a concomitant change in protein content (Hobler et al., 1999). A putative explanation for the apparent discrepancy between the response of proteasome subunits at the mRNA level and at the protein level could be an increased rate of turnover of the proteasome subunits. Alternatively, it has also been hypothesized that increased mRNA levels of proteasome subunits are required for the increased biogenesis of muscle proteasomes in acute diabetes to change the proteasome subtype pattern and modulate peptidase activities (Merforth, Kuehn, Osmers, & Dahlmann, 2003).

The 20S proteasome contains at least five peptidase activities, i.e. the trypsin-, chymotrypsin-, caspase-like, branched-chain amino acid-preferring and small neutral amino acid-preferring activities (Orlowski & Wilk, 2000, 2003). In vivo, the peptidase activities of the 20S proteasome are regulated by the 19S proteasome, which serves to recognize, unfold and inject polyubiquitinated proteins into the catalytic chamber of the 20S proteasome (Tanaka, 1995). In the present study, we measured peptidase activities of the 20S proteasome, but not of the 26S proteasome, with established methods (Fang et al., 2000; Hobler et al., 1999). To the best of our knowledge, 20S proteasome activities measured in identical or similar conditions were always in good agreement with rates of proteolysis. These activities increased when rates of total and/or proteasome-dependent proteolysis were increased (Combaret et al., 2004; Fang et al., 2000; Hobler et al., 1999; Smith, Mukerji, & Tisdale, 2005). Conversely peptidase activities decreased when proteolysis was attenuated after a catabolic event (Smith et al., 2005; Whitehouse & Tisdale, 2001), or when proteolysis decreased below basal levels (Tilgner et al., 2002). Increased 20S proteasome peptidase activities have been previously reported in septic muscles within 4 h after CLP (Hobler et al., 1999). Within a

shorter time frame (i.e. 2 h after zymosan injection), we observed a significant increase in the trypsin-like 20S proteasome peptidase activity. This very fast response suggests the involvement of a rapidly acting regulatory mechanism such as (de)phosphorylation of proteasome subunits. Indeed, the proteasome has multiple phosphorylation sites with dephosphorylation reducing proteasome activity (Mason, Hendil, & Rivett, 1996; Mason, Murray, Pappin, & Rivett, 1998).

While the increased proteasome activity in the acute phase was anticipated, we observed the highest activities at days 6 and 11 after zymosan injection. This prolonged increase in 20S proteasome activity is remarkable, especially at day 11, when muscle mass and CSA were clearly improving. Assuming that the high proteasome activities during recovery indeed reflect high rates of proteolysis, protein synthesis rates must be simultaneously increased to ensure net protein anabolism. Increased protein breakdown has been previously reported during muscle hypertrophy in the fowl (Laurent, Sparrow, & Millward, 1978) and during compensatory growth in response to muscle overloading in the rat (Goldspink, Garlick, & McNurlan, 1983). The high proteasome activity during recovery may suggest a role for Ub-P dependent proteolysis in the remodeling of skeletal muscle. An increased proteasome activity may be needed to remove or replace remnant proteins or atrophy-related protein isoforms during recovery. A role of the Ub-P pathway in muscle remodeling has been reported previously during reloading of the unweighted soleus muscle (Taillandier, Aurousseau, Combaret, Guezennec, & Attaix, 2003; Taillandier et al., 2004). Therefore, contrasting with the established role of the Ub-P system in catabolic phases, high proteasome activities may also contribute to accelerate muscle recovery. If this is the case, blocking proteasome activity for sustained periods of time could be deleterious as this may impede muscle recovery after a catabolic event.

Despite the presence of muscle atrophy, the proteasome peptidase activities and formation of ubiquitin-conjugates (except for day 2) were not increased in the pair-fed rats. This is presumably due to the stage of maturation of the rats used in this study (10 weeks at the onset of the study). Young rats exhibit a pronounced activation of the Ub-P system upon starvation (Kee et al., 2003), but this catabolic response is strongly attenuated or delayed in older (young)–adult

animals (Dehoux et al., 2004; Goodman, McElaney, & Ruderman, 1981; Mosoni et al., 1999).

In summary, the present study clearly shows an activation of the Ub-P pathway during the long-lasting muscle wasting in zymosan-injected septic rats. More interestingly, 20S proteasome peptidase activities remained elevated when muscle mass and CSA improved during the subsequent recovery period. This suggests that increased proteolysis plays a role in muscle recovery and/or remodeling.

Acknowledgement

We would like to thank Dr. S. Wing (McGill University, Montréal, Canada) for providing us with the 14-kDa E2 antibody.

References

- Attaix, D., Combaret, L., Kee, A. J., & Taillandier, D. (2003). Mechanisms of ubiquitination and proteasome-dependent proteolysis in skeletal muscle. In J. Zempleni & H. Daniels (Eds.), *Molecular nutrition* (pp. 219–235). Wallingford, Oxon, UK: CAB International.
- Chai, J., Wu, Y., & Sheng, Z. (2002). The relationship between skeletal muscle proteolysis and ubiquitin-proteasome proteolytic pathway in burned rats. *Burns*, 28(6), 527–533.
- Combaret, L., Taillandier, D., Dardevet, D., Bechet, D., Ralliere, C., Claustre, A., et al. (2004). Glucocorticoids regulate mRNA levels for subunits of the 19S regulatory complex of the 26S proteasome in fast-twitch skeletal muscles. *Biochem J*, 378(Pt. 1), 239–246.
- Dehoux, M., Van Beneden, R., Pasko, N., Lause, P., Verniers, J., Underwood, L., et al. (2004). Role of the insulin-like growth factor I decline in the induction of atrogen-1/MAFbx during fasting and diabetes. *Endocrinology*, 145(11), 4806–4812.
- Deval, C., Mordier, S., Obled, C., Bechet, D., Combaret, L., Attaix, D., et al. (2001). Identification of cathepsin L as a differentially expressed message associated with skeletal muscle wasting. *Biochem J*, 360(Pt. 1), 143–150.
- Fang, C. H., Li, B. G., Fischer, D. R., Wang, J. J., Runnels, H. A., Monaco, J. J., et al. (2000). Burn injury upregulates the activity and gene expression of the 20S proteasome in rat skeletal muscle. *Clin Sci (Lond)*, 99(3), 181–187.
- Goldspink, D. F., Garlick, P. J., & McNurlan, M. A. (1983). Protein turnover measured in vivo and in vitro in muscles undergoing compensatory growth and subsequent denervation atrophy. *Biochem J*, 210(1), 89–98.
- Goodman, M. N., McElaney, M. A., & Ruderman, N. B. (1981). Adaptation to prolonged starvation in the rat: Curtailment of skeletal muscle proteolysis. *Am J Physiol*, 241(4), E321–327.

- Hobler, S. C., Williams, A., Fischer, D., Wang, J. J., Sun, X., Fischer, J. E., et al. (1999). Activity and expression of the 20S proteasome are increased in skeletal muscle during sepsis. *Am J Physiol*, 277(2 Pt. 2), R434–440.
- Jagoe, R. T., & Goldberg, A. L. (2001). What do we really know about the ubiquitin-proteasome pathway in muscle atrophy? *Curr Opin Clin Nutr Metab Care*, 4(3), 183–190.
- Kee, A. J., Combaret, L., Tilignac, T., Souweine, B., Auroousseau, E., Dalle, M., et al. (2003). Ubiquitin-proteasome-dependent muscle proteolysis responds slowly to insulin release and refeeding in starved rats. *J Physiol*, 546(Pt. 3), 765–776.
- Laemmli, U. K. (1970). Cleavage of structural proteins during the assembly of the head of bacteriophage T4. *Nature*, 227(5259), 680–685.
- Laurent, G. J., Sparrow, M. P., & Millward, D. J. (1978). Turnover of muscle protein in the fowl. Changes in rates of protein synthesis and breakdown during hypertrophy of the anterior and posterior latissimus dorsi muscles. *Biochem J*, 176(2), 407–417.
- Lecker, S. H., Jagoe, R. T., Gilbert, A., Gomes, M., Baracos, V., Bailey, J., et al. (2004). Multiple types of skeletal muscle atrophy involve a common program of changes in gene expression. *Faseb J*, 18(1), 39–51.
- Lecker, S. H., Solomon, V., Mitch, W. E., & Goldberg, A. L. (1999). Muscle protein breakdown and the critical role of the ubiquitin-proteasome pathway in normal and disease states. *J Nutr*, 129(1S Suppl.), 227S–237S.
- Lecker, S. H., Solomon, V., Price, S. R., Kwon, Y. T., Mitch, W. E., & Goldberg, A. L. (1999). Ubiquitin conjugation by the N-end rule pathway and mRNAs for its components increase in muscles of diabetic rats. *J Clin Invest*, 104(10), 1411–1420.
- Mason, G. G., Hendil, K. B., & Rivett, A. J. (1996). Phosphorylation of proteasomes in mammalian cells. Identification of two phosphorylated subunits and the effect of phosphorylation on activity. *Eur J Biochem*, 238(2), 453–462.
- Mason, G. G., Murray, R. Z., Pappin, D., & Rivett, A. J. (1998). Phosphorylation of ATPase subunits of the 26S proteasome. *FEBS Lett*, 430(3), 269–274.
- Merforth, S., Kuehn, L., Osmers, A., & Dahlmann, B. (2003). Alteration of 20S proteasome-subtypes and proteasome activator PA28 in skeletal muscle of rat after induction of diabetes mellitus. *Int J Biochem Cell Biol*, 35(5), 740–748.
- Minnaard, R., Drost, M. R., Wagenmakers, A. J., van Kranenburg, G. P., Kuipers, H., & Hesselink, M. K. (2005). Skeletal muscle wasting and contractile performance in septic rats. *Muscle Nerve*, 31(3), 339–348.
- Mosoni, L., Malmezat, T., Valluy, M. C., Houlier, M. L., Attaix, D., & Mirand, P. P. (1999). Lower recovery of muscle protein lost during starvation in old rats despite a stimulation of protein synthesis. *Am J Physiol*, 277(4 Pt. 1), E608–616.
- Orlowski, M., & Wilk, S. (2000). Catalytic activities of the 20S proteasome, a multicatalytic proteinase complex. *Arch Biochem Biophys*, 383(1), 1–16.
- Orlowski, M., & Wilk, S. (2003). Ubiquitin-independent proteolytic functions of the proteasome. *Arch Biochem Biophys*, 415(1), 1–5.
- Pickart, C. M. (2001). Mechanisms underlying ubiquitination. *Annu Rev Biochem*, 70, 503–533.
- Price, S. R. (2003). Increased transcription of ubiquitin-proteasome system components: Molecular responses associated with muscle atrophy. *Int J Biochem Cell Biol*, 35(5), 617–628.
- Rooyackers, O. E., Saris, W. H., Soeters, P. B., & Wagenmakers, A. J. (1994). Prolonged changes in protein and amino acid metabolism after zymosan treatment in rats. *Clin Sci (Lond)*, 87(5), 619–626.
- Smith, H. J., Mukerji, P., & Tisdale, M. J. (2005). Attenuation of proteasome-induced proteolysis in skeletal muscle by {beta}-hydroxy-{beta}-methylbutyrate in cancer-induced muscle loss. *Cancer Res*, 65(1), 277–283.
- Solomon, V., Baracos, V., Sarraf, P., & Goldberg, A. L. (1998). Rates of ubiquitin conjugation increase when muscles atrophy, largely through activation of the N-end rule pathway. *Proc Natl Acad Sci USA*, 95(21), 12602–12607.
- Taillandier, D., Auroousseau, E., Combaret, L., Guezennec, C. Y., & Attaix, D. (2003). Regulation of proteolysis during reloading of the unweighted soleus muscle. *Int J Biochem Cell Biol*, 35(5), 665–675.
- Taillandier, D., Combaret, L., Pouch, M. N., Samuels, S. E., Bechet, D., & Attaix, D. (2004). The role of ubiquitin-proteasome-dependent proteolysis in the remodelling of skeletal muscle. *Proc Nutr Soc*, 63(2), 357–361.
- Tanaka, K. (1995). Molecular biology of proteasomes. *Mol Biol Rep*, 21(1), 21–26.
- Tiao, G., Hobler, S., Wang, J. J., Meyer, T. A., Luchette, F. A., Fischer, J. E., et al. (1997). Sepsis is associated with increased mRNAs of the ubiquitin-proteasome proteolytic pathway in human skeletal muscle. *J Clin Invest*, 99(2), 163–168.
- Tilignac, T., Temparis, S., Combaret, L., Taillandier, D., Pouch, M. N., Cervek, M., et al. (2002). Chemotherapy inhibits skeletal muscle ubiquitin-proteasome-dependent proteolysis. *Cancer Res*, 62(10), 2771–2777.
- Voisin, L., Breuille, D., Combaret, L., Pouyet, C., Taillandier, D., Auroousseau, E., et al. (1996). Muscle wasting in a rat model of long-lasting sepsis results from the activation of lysosomal, Ca²⁺-activated, and ubiquitin-proteasome proteolytic pathways. *J Clin Invest*, 97(7), 1610–1617.
- Whitehouse, A. S., & Tisdale, M. J. (2001). Downregulation of ubiquitin-dependent proteolysis by eicosapentaenoic acid in acute starvation. *Biochem Biophys Res Commun*, 285(3), 598–602.